# A Fingerprint Recognition Algorithm Using Phase-Based Image Matching for Low-Quality Fingerprints

Koichi Ito†, Ayumi Morita†, Takafumi Aoki†, Tatsuo Higuchi‡, Hiroshi Nakajima$, and Koji Kobayashi$

† Graduate School of Information Sciences, Tohoku University,
Sendai-shi 980-8579, Japan
E-mail: ito@aoki.ecei.tohoku.ac.jp
‡ Faculty of Engineering, Tohoku Institute of Technology, Sendai-shi 982-8577, Japan
$ Yamatake Corporation, Isehara-shi 259-1195, Japan

**Abstract— A major approach for fingerprint recognition today is to extract minutiae from fingerprint images and to perform fingerprint matching based on the number of corresponding minutiae pairings. One of the most difficult problems in fingerprint recognition has been that the recognition performance is significantly influenced by fingertip surface condition, which may vary depending on environmental or personal causes. Addressing this problem, this paper presents a fingerprint recognition algorithm using phase-based image matching. The use of phase components in 2D (two-dimensional) discrete Fourier transforms of fingerprint images makes possible to achieve highly robust fingerprint recognition for low-quality fingerprints. Experimental evaluation using a set of fingerprint images captured from fingertips with difficult conditions (e.g., dry fingertips, rough fingertips, allergic-skin fingertips) demonstrates an efficient recognition performance of the proposed algorithm compared with a typical minutiae-based algorithm.**

## I. Introduction

Biometric authentication has been receiving extensive attention over the past decade with increasing demands in automated personal identification. Biometrics is to identify individuals using physiological or behavioral characteristics, such as fingerprint, face, iris, retina, palm-print, etc. Among all the biometric techniques, fingerprint recognition [1] is the most popular method and is successfully used in many applications.

Typical fingerprint recognition methods employ feature-based image matching, where minutiae (i.e., ridge ending and ridge bifurcation) are extracted from the registered fingerprint image and the input fingerprint image, and the number of corresponding minutiae pairings between the two images is used to recognize a valid fingerprint image [1]. The feature-based matching provides an effective way of identification for majority of people.

However, it has been known that there are a number of people whose fingerprints could not be identified by the feature-based methods due to special skin conditions, where feature points are hard to be extracted by image processing. The ratio of people who have such difficult fingerprints varies depending on race, sex, age, job groupings, etc., but it is said that one to five percentage of total population may fall into this category.

Addressing this problem, this paper proposes an efficient fingerprint recognition algorithm using phase-based image matching — an image matching technique using the phase components in 2D Discrete Fourier Transforms (DFTs) of given images. The technique has been successfully applied to high-accuracy image registration tasks for computer vision applications [2]–[4], where estimation of sub-pixel image translation is a major concern. In this paper, we demonstrate that this technique is highly effective also for fingerprint matching (see [5] for earlier discussions on this idea). The use of Fourier phase information of fingerprint images makes possible highly reliable fingerprint matching for low-quality fingerprints whose minutiae are difficult to be extracted.

## II. Phase-Based Image Matching

In this section, we introduce the principle of phase-based image matching using the Phase-Only Correlation (POC) function (which is sometimes called the "phase-correlation function") [2]–[4]. Consider two $N_1 \times N_2$ images, $f(n_1, n_2)$ and $g(n_1, n_2)$, where we assume that the index ranges are $n_1 = -M_1 \cdots M_1$ ($M_1 > 0$) and $n_2 = -M_2 \cdots M_2$ ($M_2 > 0$) for mathematical simplicity, and hence $N_1 = 2M_1 + 1$ and $N_2 = 2M_2 + 1$. Let $F(k_1, k_2)$ and $G(k_1, k_2)$ denote the 2D DFTs of the two images. $F(k_1, k_2)$ is given by

$$F(k_1, k_2) = \sum_{n_1, n_2} f(n_1, n_2) W_{N_1}^{k_1 n_1} W_{N_2}^{k_2 n_2}$$

0-7803-9134-9/05/$20.00 ©2005 IEEE

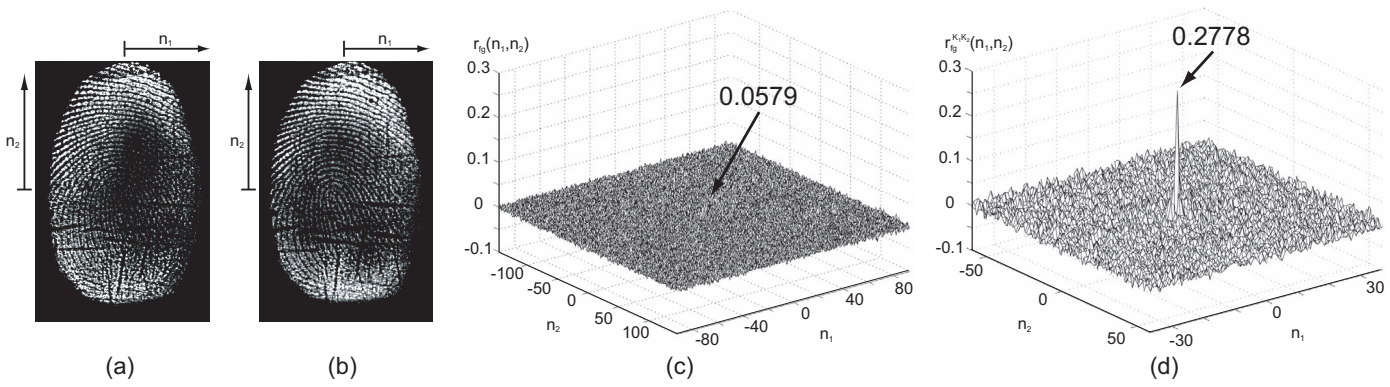


Fig. 1. Example of genuine matching using the original POC function and the BLPOC function: (a) registered fingerprint image $f(n_1, n_2)$, (b) input fingerprint image $g(n_1, n_2)$, (c) original POC function $r_{fg}(n_1, n_2)$ and (d) BLPOC function $r_{fg}^{K_1 K_2}(n_1, n_2)$ with $K_1 = 34$ and $K_2 = 63$.

$$= A_F(k_1, k_2) e^{j\theta_F(k_1,k_2)}, \quad (1)$$

where $k_1 = -M_1 \cdots M_1$, $k_2 = -M_2 \cdots M_2$, $W_{N_1} = e^{-j\frac{2\pi}{N_1}}$, $W_{N_2} = e^{-j\frac{2\pi}{N_2}}$, and $\sum_{n_1,n_2}$ denotes $\sum_{n_1=-M_1}^{M_1} \sum_{n_2=-M_2}^{M_2}$. $A_F(k_1, k_2)$ is amplitude and $\theta_F(k_1, k_2)$ is phase. $G(k_1, k_2)$ is defined in the same way. The cross-phase spectrum $R_{FG}(k_1, k_2)$ is given by

$$R_{FG}(k_1, k_2) = \frac{F(k_1, k_2)\overline{G(k_1, k_2)}}{|F(k_1, k_2)\overline{G(k_1, k_2)}|} = e^{j\theta(k_1,k_2)}, \quad (2)$$

where $\overline{G(k_1, k_2)}$ is the complex conjugate of $G(k_1, k_2)$ and $\theta(k_1, k_2)$ denotes the phase difference $\theta_F(k_1, k_2) - \theta_G(k_1, k_2)$. The POC function $r_{fg}(n_1, n_2)$ is the 2D Inverse DFT (2D IDFT) of $R_{FG}(k_1, k_2)$ and is given by

$$r_{fg}(n_1, n_2) = \frac{1}{N_1 N_2} \sum_{k_1,k_2} R_{FG}(k_1, k_2) W_{N_1}^{-k_1 n_1} W_{N_2}^{-k_2 n_2}, \quad (3)$$

where $\sum_{k_1,k_2}$ denotes $\sum_{k_1=-M_1}^{M_1} \sum_{k_2=-M_2}^{M_2}$. When two images are similar, their POC function gives a distinct sharp peak. When two images are not similar, the peak drops significantly. The height of the peak gives a good similarity measure for image matching, and the location of the peak shows the translational displacement between the images.

We modify the definition of POC function to have a BLPOC (Band-Limited Phase-Only Correlation) function dedicated to fingerprint matching tasks. The idea to improve the matching performance is to eliminate meaningless high frequency components in the calculation of cross-phase spectrum $R_{FG}(k_1, k_2)$ depending on the inherent frequency components of fingerprint images [5]. Assume that the ranges of the inherent frequency band are given by $k_1 = -K_1 \cdots K_1$ and $k_2 = -K_2 \cdots K_2$, where $0 \leq K_1 \leq M_1$ and $0 \leq K_2 \leq M_2$. Thus, the effective size of frequency spectrum is given by $L_1 = 2K_1 + 1$ and $L_2 = 2K_2 + 1$. The BLPOC function is given by

$$r_{fg}^{K_1 K_2}(n_1, n_2) = \frac{1}{L_1 L_2} {\sum_{k_1,k_2}}' R_{FG}(k_1, k_2) \times W_{L_1}^{-k_1 n_1} W_{L_2}^{-k_2 n_2}, \quad (4)$$

where $n_1 = -K_1 \cdots K_1$, $n_2 = -K_2 \cdots K_2$, and $\sum'_{k_1,k_2}$ denotes $\sum_{k_1=-K_1}^{K_1} \sum_{k_2=-K_2}^{K_2}$. Note that the maximum value of the correlation peak of the BLPOC function is always normalized to 1 and does not depend on $L_1$ and $L_2$.

Figure 1 shows an example of genuine matching using the original POC function $r_{fg}$ and the BLPOC function $r_{fg}^{K_1 K_2}$. The BLPOC function provides the higher correlation peak and better discrimination capability than that of the original POC function.

## III. Fingerprint Recognition Algorithm

In this section, we propose the fingerprint recognition algorithm using the POC function. Figure 2 shows the flow diagram of the proposed fingerprint recognition algorithm. The proposed algorithm consists of the four steps: (i) core detection, (ii) rotation and displacement alignment, (iii) common region extraction and (iv) fingerprint matching.

**(i) Core detection**

This step is to detect the core of the registered fingerprint image $f(n_1, n_2)$ and the input fingerprint image $g(n_1, n_2)$ in order to align the displacement between the two images. The core is defined as a singular point in a fingerprint image that exhibits the maximum ridge line curvature. The Poincaré index method [6] is used to detect the core in our system.

**(ii) Displacement and rotation alignment**

We need to normalize the displacement and the rotation between the registered fingerprint $f(n_1, n_2)$ and the input fingerprint $g(n_1, n_2)$ in order to perform the high-accuracy fingerprint matching.

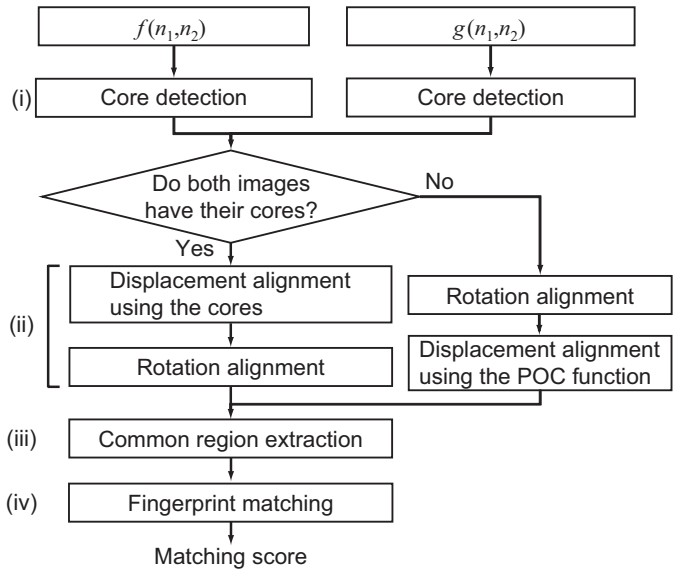


Fig. 2. Flow diagram of the proposed algorithm.

In the case when both fingerprint images have their cores, we first align the translational displacement between fingerprint images using the position of the cores. Next, we normalize the rotation by using a straightforward approach as follows. We first generate a set of rotated images $f_\theta(n_1, n_2)$ of the registered fingerprint $f(n_1, n_2)$ over the angular range $-40^\circ \leq \theta \leq 40^\circ$ with an angle spacing $1^\circ$, where bi-cubic interpolation is employed for image rotation. The rotation angle $\Theta$ of the input image relative to the registered image can be determined by evaluating the similarity between the rotated replicas of the registered image $f_\theta(n_1, n_2)$ ($-40^\circ \leq \theta \leq 40^\circ$) and the input image $g(n_1, n_2)$ using the BLPOC function.

When either $f(n_1, n_2)$ or $g(n_1, n_2)$ does not have its core, we first normalize the rotation by the above straightforward approach. Next, we align the translational displacement between the rotation-normalized image $f_\Theta(n_1, n_2)$ and the input image $g(n_1, n_2)$. The displacement can be obtained as the peak location of the POC function between $f_\Theta(n_1, n_2)$ and $g(n_1, n_2)$.

Thus, we have normalized versions of the registered image and the input image, which are denoted by $f'(n_1, n_2)$ and $g'(n_1, n_2)$.

**(iii) Common region extraction**

Next step is to extract the overlapped region (intersection) of the two images $f'(n_1, n_2)$ and $g'(n_1, n_2)$. This process improves the accuracy of fingerprint matching, since the non-overlapped areas of the two images become the uncorrelated noise components in the BLPOC function. In order to detect the effective fingerprint areas in the registered image $f'(n_1, n_2)$ and the input image $g'(n_1, n_2)$, we examine the $n_1$-axis projection and the $n_2$-axis projection of pixel values. Only the common effective image areas, $f''(n_1, n_2)$ and $g''(n_1, n_2)$, with the same size are extracted for the succeeding image matching step.

**(iv) Fingerprint matching**

We calculate the BLPOC function $r^{K_1 K_2}_{f'' g''}(n_1, n_2)$ between the two extracted images $f''(n_1, n_2)$ and $g''(n_1, n_2)$, and evaluate the matching score. The BLPOC function may give multiple correlation peaks due to elastic fingerprint deformation. Thus, we define the matching score between the two images as the sum of the highest two peaks of the BLPOC function $r^{K_1 K_2}_{f'' g''}(n_1, n_2)$.

## IV. Experimental Results

This section describes a set of experiments for evaluating fingerprint matching performance of the proposed algorithm.

In our experiment, the database consists of impressions obtained from 30 subjects using a pressure sensitive sensor (BLP-100, BMF Corporation), which can capture fingerprint images of $256 \times 384$ pixels. In the captured images, 20 of subjects have good-quality fingerprints and the remaining 10 subjects have low-quality fingerprints due to dry fingertips (6 subjects), rough fingertips (2 subjects) and allergic-skin fingertips (2 subjects). Figure 3 shows some examples of fingerprint images. Thus, the test set considered here is specially designed to evaluate the performance of fingerprint matching under difficult condition. We capture 11 impressions of the right index finger for every subject, each of which is taken at different timing. The total number of fingerprint images used in this experiment is 330 (30 subjects $\times$ 11 images).

We compare three different matching algorithms: (A) a typical minutiae-based algorithm (which is commercially available), (B) a simple POC-based algorithm [5], and (C) the proposed algorithm. The performance of the biometrics-based identification system is evaluated by the Receiver Operating Characteristic (ROC) curve, which illustrates the False Non-Matching Rate (FNMR) against the False Matching Rate (FMR) at different thresholds on the matching score. We first evaluate the FNMR for all possible combinations of genuine attempts; the number of attempts is ${}_{11}C_2 \times 30 = 1650$. Next, we evaluate the FMR for ${}_{30}C_2 = 435$ impostor attempts, where we select a single image (the first image) for each fingerprint and make all the possible combinations of impostor attempts. Figure 4 shows the ROC curve for the three algorithms (A)–(C). The proposed algorithm (C) exhibits significantly higher performance, since its ROC curve is located at lower FMR/FNMR region than those of the minutiae-based algorithm (A) and the POC-based algorithm (B).

The Equal Error Rate (EER) and the ZeroFMR are used to summarize the accuracy of a verification system. The EER is defined as the error rate where the FNMR and the FMR are equal. The ZeroFMR is defined as the lowest FNMR where FMR=0%. Table I summarizes EER and ZeroFMR for matching attempts using all the fingerprints and for attempts using only low-quality fingerprints. In the case of using all the fingerprints, the EER of the proposed algorithm (C) is 1.90%, while the EER of the POC-based algorithm (B) is 3.03% and that of


Fig. 3. Examples of fingerprint images in the database: (a) good-quality fingerprint, (b) dry fingertip, (c) rough fingertip and (d) allergic-skin fingertip.

the minutiae-based algorithm (A) is 4.81%. In the case of using only low-quality fingerprints, the EER of the proposed algorithm (C) is 0.00%, while the EER of POC-based algorithm (B) is 0.54% and that of the minutiae-based algorithm (A) is 10.31%. As is observed in the above experiments, the proposed algorithm is particularly useful for verifying low-quality fingerprints.

## V. Conclusion

This paper proposed an efficient fingerprint recognition algorithm using the phase-based image matching. The proposed technique is particularly effective for verifying low-quality fingerprint images that could not be identified correctly by conventional techniques. We developed commercial fingerprint verification units for access control applications [7]. We expect that the proposed technique is implemented in existing fingerprint verification units in the near future.

## References

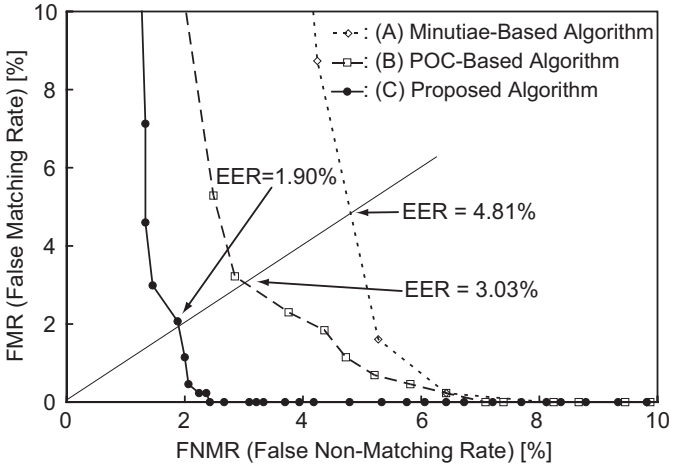


Fig. 4. ROC curves and EER.

TABLE I. ZeroFMR and EER for matching attempts using all the fingerprints and for matching attempts using only low-quality fingerprints.

| | All Fingerprints (30 subjects × 11 images) | | Low-Quality Fingerprints (10 subjects × 11 images) | |
|---|---|---|---|---|
| | ZeroFMR | EER | ZeroFMR | EER |
| (A) | 8.12% | 4.81% | 13.64% | 10.31% |
| (B) | 7.09% | 3.03% | 0.54% | 0.54% |
| (C) | 2.42% | 1.90% | 0.00% | 0.00% |

[1] D. Maltoni, D. Maio, A. K. Jain, and S. Prabhakar, *Handbook of Fingerprint Recognition*. Springer, 2003.

[2] C. D. Kuglin and D. C. Hines, "The phase correlation image alignment method," *Proc. Int. Conf. on Cybernetics and Society*, pp. 163–165, 1975.

[3] K. Takita, T. Aoki, Y. Sasaki, T. Higuchi, and K. Kobayashi, "High-accuracy subpixel image registration based on phase-only correlation," *IEICE Trans. Fundamentals*, vol. E86-A, no. 8, pp. 1925–1934, Aug. 2003.

[4] K. Takita, M. A. Muquit, T. Aoki, and T. Higuchi, "A subpixel correspondence search technique for computer vision applications," *IEICE Trans. Fundamentals*, vol. E87-A, no. 8, pp. 1913–1923, Aug. 2004.

[5] K. Ito, H. Nakajima, K. Kobayashi, T. Aoki, and T. Higuchi, "A fingerprint matching algorithm using phase-only correlation," *IEICE Trans. Fundamentals*, vol. E87-A, no. 3, pp. 682–691, Mar. 2004.

[6] M. Kawagoe and A. Tojo, "Fingerprint pattern classification," *Pattern Recognition*, vol. 17, no. 3, pp. 295–303, 1984.

[7] Products using phase-based image matching. [Online]. Available: http://www.aoki.ecei.tohoku.ac.jp/poc/